

Citation for published version:

Ding, W, Gorbach, AV, Wadsworth, WJ, Knight, JC, Skryabin, DV, Strain, MJ, Sorel, M & De La Rue, RM 2011, Time- and frequency-domain measurements of solitons in subwavelength silicon waveguides using cross-correlation. in *2011 Conference on Lasers and Electro-Optics: Laser Science to Photonic Applications, CLEO 2011.*, QFF2, IEEE, Piscataway, NJ, 2011 Conference on Lasers and Electro-Optics, CLEO 2011, May 1, 2011 - May 6, 2011, Baltimore, MD, USA United States, 1/05/11.

Publication date:
2011

Document Version
Peer reviewed version

[Link to publication](#)

© 2011 IEEE. Personal use of this material is permitted. Permission from IEEE must be obtained for all other uses, in any current or future media, including reprinting/republishing this material for advertising or promotional purposes, creating new collective works, for resale or redistribution to servers or lists, or reuse of any copyrighted component of this work in other works

University of Bath

General rights

Copyright and moral rights for the publications made accessible in the public portal are retained by the authors and/or other copyright owners and it is a condition of accessing publications that users recognise and abide by the legal requirements associated with these rights.

Take down policy

If you believe that this document breaches copyright please contact us providing details, and we will remove access to the work immediately and investigate your claim.

Time- and Frequency-Domain Measurements of Solitons in Subwavelength Silicon Waveguides Using Cross-correlation

W. Ding,^{1*} A.V. Gorbach,¹ W.J. Wadsworth,¹ J.C. Knight,¹ D.V. Skryabin,¹ M.J. Strain,² M. Sorel,² and R.M. De La Rue²

¹Centre for Photonics and Photonic Materials, Department of Physics, University of Bath, Bath BA2 7AY, UK

²Department of Electronics and Electrical Engineering, University of Glasgow, Glasgow G12 8LT, UK

*Email: w.ding@bath.ac.uk

Abstract: Time-domain measurements of dispersion- and nonlinearity-induced chirpings of femtosecond pulses in silicon-on-insulator nanowires reveal nonlinear dispersion compensation. Spectral measurements show pronounced dispersive wave emission by solitons.

OCIS codes: 130.4310, 190.5530, 190.4390, 130.2790

Silicon photonics has attracted much attention due to potential applications in photonic circuitry [1]. The large index contrast between silicon and other materials and the strong third-order nonlinearities of silicon can be used to realize a variety of on-chip nonlinear functions [1]. While spectral measurements of nonlinear processes in subwavelength waveguides have been well reported, time-domain or simultaneous time-and-frequency characterization is required to fully characterize such effects as soliton formation, pulse compression and more complex process [2]. In this work, we investigate soliton formation in silicon-on-insulator (SOI) waveguides by observing it in frequency and time domains by using cross-correlation.

A 220 nm thick, 380 nm wide and 3.4 mm long waveguide was fabricated using electron beam lithography and inductively coupled plasma reactive ion etching. Its group velocity dispersion was measured as described in [3]. At the wavelength of 1.56 μm , which is the carrier wavelength of our pump pulses, the waveguide has anomalous group velocity dispersion (GVD), $\beta_2 = -3.01 \pm 0.10 \text{ ps}^2/\text{m}$, and 3rd order dispersion $\beta_3 = -0.070 \pm 0.002 \text{ ps}^3/\text{m}$, with zero GVD at $\lambda=1600 \text{ nm}$. Fig. 1a shows our experimental setup for nonlinear measurements. An Erbium-doped fiber ring laser produces an ultrashort pulse train at 1.56 μm with a repetition rate of 33 MHz. This pulse train is passed through a band-pass filter to remove spectral sidebands. After filtering, the ultrashort pulses are sent into a chirped-pulse Erbium-doped fiber amplifier (EDFA). Using an auto-correlator at the exit of the EDFA (insert in Fig. 1a), we measure the full width of the pulse at half maximum of its intensity (FWHM) to be $T_{fwhm} = 175 \text{ fs}$. The chirp of this pulse is modest, assuming a sech pulse shape. In our setup, several polarizing cubes are used to constrain the polarization to be parallel to the substrate (TE mode), and a 5% plate beam splitter is used to construct the reference arm of the cross-correlator. The pulse train is then coupled into the SOI waveguide through an AR-coated singlet lens (numerical aperture, NA = 0.65) with the estimated coupling coefficient of 12 dB. Pulses at the waveguide output are characterized using either an optical spectral analyzer or a cross-correlator.

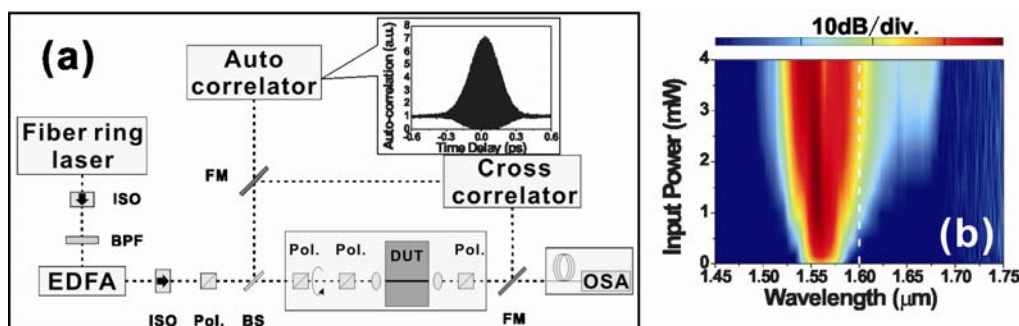


Fig. 1. (a) Experimental setup. ISO: isolator; BPF: band-pass filter; Pol.: polarizer; BS: beam splitter; DUT: device under test; FM: flip mirror. (b) Measured output spectra with increasing input power (log scale). The vertical dashed line stands for zero-GVD wavelength.

Fig. 1b shows the output spectrum as a function of the input power, i.e., the average power before the coupling lens. When power is above the soliton threshold, the spectrum develops pronounced asymmetry due to the peak growing at around 1670 nm in the range of normal GVD. We attribute this peak to the Cherenkov radiation emitted by the solitons [2,4]. The wavelength of the Cherenkov resonance can be predicted by matching the propagation constant of the linear dispersive wave to the propagation constant of a soliton [2]. Assuming the soliton carrier wavelength to be in the range from 1.5 to 1.55 μm , we find that the Cherenkov radiation should appear between 1.625 and 1.690 μm , in agreement with our measurements (Fig. 1b).

To demonstrate the soliton formation process, we use cross-correlation based on the sum of the signal field

$E_s=A_s(t)e^{-i\omega t} + c.c.$ (pulse after the waveguide) and of the reference field $E_r=A_r(t)e^{-i\omega t} + c.c.$ (input pulse). The corresponding cross-correlation integral is $I_c(\tau) = R \int [E_r(t) + E_s(t + \tau)]^4 dt$, where τ is the time delay and R is the repetition rate. We measure weak signals by exploiting a strong reference pulse in the cross-correlator. We do not amplify the signal, since it would unavoidably produce distortions. Using relatively high repetition rates helps to improve the measured signal, which partly motivates our choice of a fiber ring laser having $R = 33$ MHz.

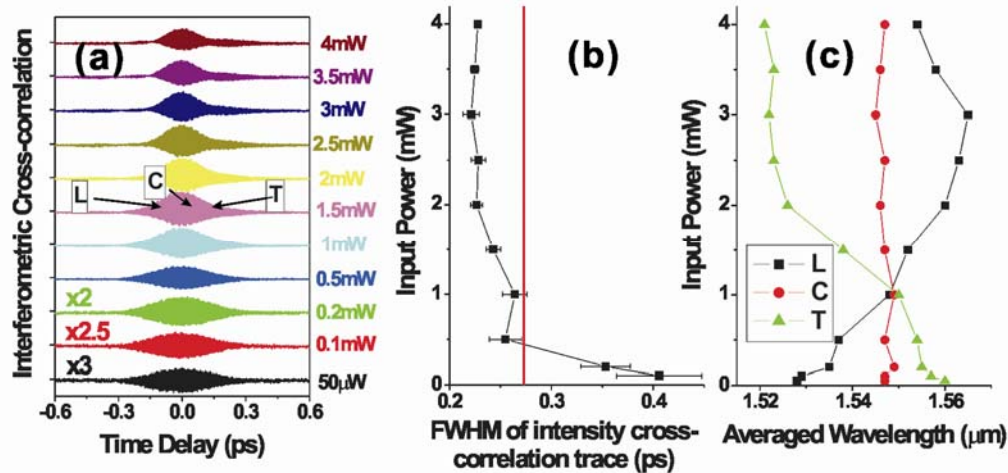


Fig. 2. (a) Measured interferometric cross-correlation traces with increasing input powers. The bottom three curves are multiplied by 3, 2.5, and 2 respectively for clarity. The symbols L, C, and T represent the leading, central, and trailing regions of the pulse. (b) FWHM of intensity cross-correlation traces vs input power. The red line stands for the FWHM of the intensity auto-correlation trace of the input pulse. (c) Averaged wavelength in the leading (black), central (red), and trailing (green) regions of the interferometric cross-correlation traces vs input power.

At low input powers, GVD will be the dominant factor determining the frequency chirp. The dispersion length L_d of a sech input pulse, $sech(t/T_0)$, is defined as $L_d = T_0^2/|\beta_2| = 3.3$ mm, where $T_{fwhm} = 2\ln(1 + \sqrt{2})T_0$. Thus L_d of the input pulse is comparable to the waveguide length, 3.4 mm, and temporal broadening and GVD-induced chirp of the transmitted pulses in the linear regime should be noticeable. Fig. 2a shows measured interferometric cross-correlation traces with increasing input powers and Fig. 2b shows how the FWHM of the intensity cross-correlation trace varies with power. Fast oscillations of I_c provide direct information about distribution of the signal frequency across the pulse profile. We equally divide every trace into the leading, central, and trailing regions and measure the averaged wavelength by counting the distance corresponding to 16 continuous oscillations in every region. At low input powers, the leading region of the pulse is bluer than the trailing one (see Fig. 2c), which is consistent with the anomalous GVD. Comparing Figs. 2b and 2c, one can see that the GVD-induced chirping is directly associated with the pulse broadening in time domain. As the input power increases, nonlinearity-induced chirp starts balancing the GVD chirping. These two effects become equal at around 1 mW of the average input power, which corresponds to the soliton formation threshold in our system. Relating the average input power P_{av} to the peak power inside the waveguide P , we find the threshold of soliton formation to be $P \approx 7W$. From numerical modeling [4], we have determined that the output pulse is compressed to around $T_0=60$ fs under these conditions (our measurements are limited by the reference pulse length), and the nonlinear parameter of the waveguide $\gamma \approx |\beta_2|/T_0^2/P \approx 120$ [Wm] $^{-1}$. Increasing the power, we observe that the further chirping of the pulse is determined by the Kerr nonlinearity, i.e., the leading region of the pulse becomes redder than the trailing one (Fig. 2c).

In summary, we have observed how the GVD-induced chirping of the low power femtosecond pulses is compensated by the opposing nonlinearity-induced chirping at higher powers, providing direct experimental verification of the main physical principle of soliton formation in subwavelength silicon waveguides.

References

- [1]. J. Leuthold, C. Koos and W. Freude, "Nonlinear silicon photonics", Nat. Photonics 4, 535-544 (2010).
- [2]. D.V. Skryabin, A.V. Gorbach, "Looking at a soliton through the prism of optical supercontinuum", Rev. Mod. Phys. 82, 1287-1299 (2010).
- [3]. W. Ding, C.J. Benton, A.V. Gorbach, W.J. Wadsworth, J.C. Knight, D.V. Skryabin, M. Gnan, M. Sorel, and R.M. De-La-Rue, "Solitons and spectral broadening in long silicon-on-insulator photonic wires", Opt. Express 16, 3310-3319 (2008).
- [4]. A.V. Gorbach, W. Ding, O.K. Staines, C.E. de Nobrega, G.D. Hobbs, W.J. Wadsworth, J.C. Knight, D.V. Skryabin, A. Samarelli, M. Sorel, and R.M. De-La-Rue, "Spatiotemporal nonlinear optics in arrays of subwavelength waveguides", Phys. Rev. A 82, 041802(R) (2010).